

Observation of Different Molecular Alignments of [Ni(salphen)] Substituted by a Different Number of Octyl Groups at HOPG Surface

Yoshinori Tamaki,^{*1} Kazuaki Tomono,² Yuki Hata,¹ Nanami Saita,¹ Takashi Yamamoto,¹ and Kazuo Miyamura^{*1}

¹Department of Chemistry, Faculty of Science, Tokyo University of Science, 1-3 Kagurazaka, Shinjuku-ku, Tokyo 162-8601

²Department of Material Chemistry, Graduate School of Science and Engineering, Yamaguchi University, 2-16-1 Tokiwadai, Ube, Yamaguchi 755-8611

Received October 17, 2011; E-mail: tamakiyoshinori99@yahoo.co.jp, miyamura@rs.kagu.tus.ac.jp

The surface adsorption structures of two Schiff-base metal complexes, [*N,N'*-bis(5-octylsalicylidene)-*o*-phenylenediaminato]nickel(II) (**1**) and [*N,N'*-bis(3,5-dioctylsalicylidene)-*o*-phenylenediaminato]nickel(II) (**2**), are imaged using scanning tunneling microscopy (STM), and compared with the dimeric structure predicted by single-crystal X-ray diffraction and NMR analyses. STM images of **1** and **2** obtained at an *o*-dichlorobenzene/HOPG interface showed that **1** was adsorbed in the form of dimers, while **2** was adsorbed as monomers at HOPG surface. The surface structure of **1** was similar to that of the reported salen complex analogue. ¹H NMR measurement revealed that the equilibrium constants of dimer formation for **1** and **2** in chloroform-*d* were determined to be $K (= [\text{dimer}]/[\text{monomer}]^2) = 14.5$ and $1.9 \text{ mol}^{-1} \text{ dm}^3$, respectively. This decreased tendency of **2** to form dimer is concluded to be the reason why **2** did not form dimers at HOPG surface. The crystal structure of **1** in which **1** is found to form dimers is also presented.

Compounds bearing both hydrophilic and hydrophobic moieties within a molecule tend to gather at liquid–liquid or liquid–solid interface, because at the interface, hydrophilic or hydrophobic properties change discontinuously. We call this nature the surface activity, and those amphiphilic compounds the surfactants. At the liquid–solid interface, surfactants gather to form self-assembled monolayers (SAMs) with characteristic structures, which are now, frequently observed by scanning tunnelling microscope (STM). Since SAMs exhibit a variety of properties and are used as catalysis,¹ chemical sensors,^{2–5} electrochemical agents,^{6,7} corrosion protecting materials,^{8–10} lubricants,^{11–15} adhesive and wetting materials,^{16–21} the relation between the structure of SAMs and their properties is intensively investigated.

Lately, in the field of coordination chemistry, the number of reports on the observation of monolayers formed by metal complexes is rapidly increasing. Metal complexes with large π -conjugated system are known to easily exchange electrons with other molecule, and by this nature, they are the good candidates of the above-mentioned functional materials. Phthalocyanine was the first metal complex observed by STM with a well-resolved molecular image.²² Since then, not only the phthalocyanines,^{23–26} but also a variety of metal complexes such as porphyrins,^{26–29} chlorophylls,^{30–32} and other metal complexes³³ have been observed by STM. We have also reported some STM images of salen [=bis(salicylidene)ethylenediaminato] complexes substituted by two alkyl side chains since 2000.^{34,35} The outstanding feature of this complex is that it assembles at interface in the form of dimers. Some related compounds imaged recently also showed the presence of

dimeric structure.³⁶ The key technology to stabilize the surface structure of complex is to introduce long alkyl chains. Alkyl chains strongly adsorb on HOPG by CH– π interaction and help to cease the movement of the molecule at HOPG surface.

In this paper is reported the change in self-assembled structures of salphen [=bis(salicylidene)-*o*-phenylenediaminato] complex analogues by the number of long alkyl chains introduced. The difference between salen and salphen is that the ethylene moiety (–CH₂–CH₂–) is changed to phenylene (–C₆H₄–), and thus the π -conjugated system is extended in salphen. We have synthesized two nickel(II) complexes of salphen substituted by two (**1**) and four (**2**) alkyl chains (Chart 1), and observed their molecular images by STM. We obtained totally different surface structures and also found that the surface structure reflects the structure they adopt in solution.

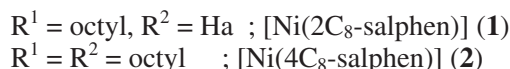
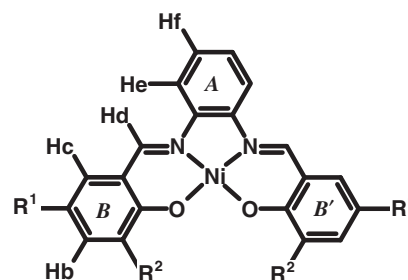


Chart 1.

Results and Discussion

STM Images. The self-assembled adlayers of **1** ([Ni(salphen)] substituted with two octyl groups) and **2** (**1** substituted with two extra octyl groups) on solid (HOPG)–liquid (*o*-dichlorobenzene; *o*-DCB) interface were observed, characterized, and imaged with STM under ambient conditions. STM image obtained at low bias voltage showed a hexagonal lattice of HOPG surface, while that at high bias showed the highly ordered self-assembled adlayer of complex molecules, indicating that the phenomenon was bias dependent.¹⁴ The molecular orbitals calculated by DFT showed that the HOMO is located at aromatic rings and Ni(II) as shown in Figure 1. This agrees with the observation that the aromatic moieties of the molecules are found to appear brighter than the other parts.

Figure 2a shows the STM image of the self-assembled adlayer of complex **1** on HOPG surface, scanned at high bias voltage; bias voltage -1.2 V, tunnel current 4.0 nA. This ordered image due to adsorbed **1** at HOPG/*o*-DCB interface was observed two days after the sample preparation. In Figure 2a, ring-like structures cover the whole domain, and

the dimension of the unit cell was 2.25×1.50 nm² with acute angle of 78° . Thus the area of unit cell was calculated to be 3.30 nm². The parameter a and a' , b and b' were the same distance ($a = a' = 2.25$ nm, $b = b' = 1.50$ nm). Figure 2b shows that the magnified STM image is composed of four bright spots being brighter than the other one. Figure 2c shows a line profile along the arrow in Figure 2c. The spot A is twice as high as A'. This strongly suggests the formation of dimer shown in Figures 2d and 2e just as that observed in crystal analyzed

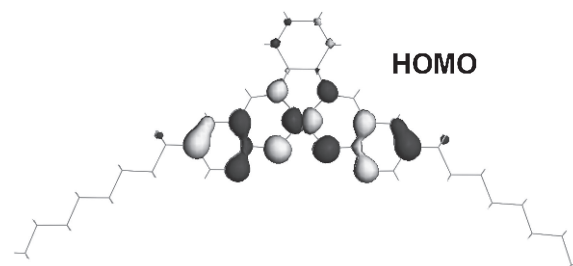


Figure 1. Optimized structure and HOMO of **1** calculated by DFT.

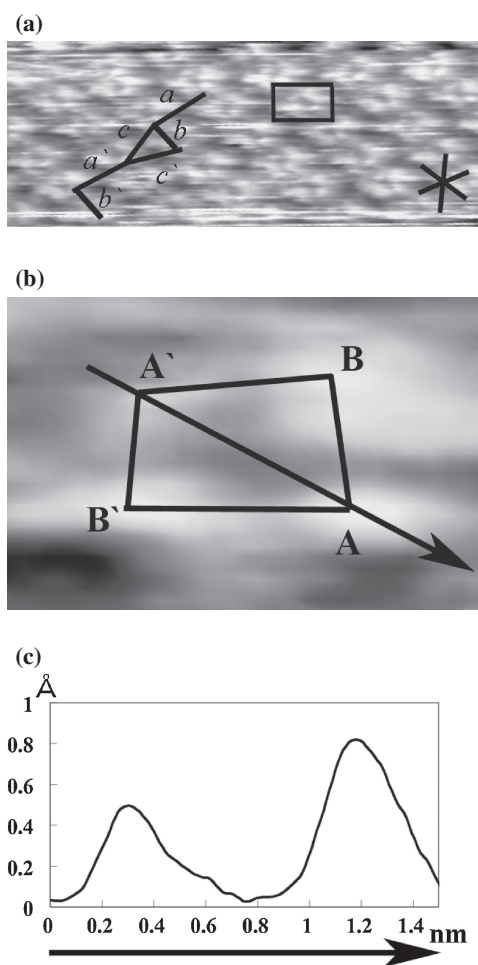


Figure 2. (a) Constant current STM image of **1** on HOPG. Area: 18.0 nm \times 7.0 nm; Bias voltage -1.2 V; tunneling current 4.0 nA. Unit cell dimensions: $a = 2.25$ nm, $b = 1.50$ nm; $\alpha = 78^\circ$. (b) Magnified STM image of area shown as a rectangle in (a). Area: 1.8 nm \times 1.2 nm. (c) Line profile over an arrow indicated in figure (b). (d) Proposed adsorbed structure model viewed from direction normal to the surface of HOPG. (e) Side view of the proposed adsorbed model of HOPG. * at right corner indicates the three axes of underlying HOPG surface from here after. Octyl chains of ball and stick model are omitted for clarity.

with X-ray crystallography given later in the text. ^1H NMR study, discussed later in the text, also revealed that **1** tends to form similar dimer. For a more quantitative representation of the data, the distance between A and B, B and B' were 0.57 and 0.88 nm, respectively. B–A–B' and B–A'–B' angles were 83 and 105°, respectively. From the results of X-ray crystallography given later in the text, the distance between the centers of aromatic rings A and B, B and B' in the scheme were 0.65 and 0.79 nm, respectively, and the angle B–A–B' was 75°. By comparing the lengths and angles, the distance between bright spots B and B' in Figure 2b could be assigned as B and B' aromatic rings of a molecule **1**. However, the facts that the distance between A and B is shorter and that the angle of B–A–B' is larger than the angle from X-ray crystallographic analysis, indicate that molecules **1** are inclined from the HOPG surface as shown in Figure 2e. The obtained dimension of dimer in Figure 2d agreed well with the dimension of the ring-like structure. We also investigated the possibility of coadsorption of complex **1** and *o*-DCB. However, the distance between the bright spots was too narrow to put *o*-DCB into space. Therefore, we concluded that the ring-like structure exhibited by **1** is of a dimer as indicated in Figure 2d and Figure 2e, and the dimers are fixed by three-point mounting of aromatic rings.

The alkyl groups are known to usually align along the underlying HOPG lattice due to the stabilization caused by CH– π interaction. Although the alkyl chains are not imaged clearly, we estimated that the alkyl groups are thus aligned. In Figure 3 is given the arrangement model of Figure 2a with van der Waals radii in accordance with the STM image. Figure 2a shows the first adsorbed layer of complex **1** on HOPG and the octyl chains lie along one of the three HOPG lattice indicated in lower right corner. The metal–metal distance along *a* axis corresponds to the sum of the length of a salphen and an octyl group. This fact suggests that the alkyl chains are aligned along one of the HOPG lattices with the octyl groups being interdigitated as shown in Figure 2a. In Figure 2a, we found a declination of *a* axis indicated by *c* and *c'* axes (*c* = 2.02 nm and *c'* = 2.30 nm). This defect can be explained by the difference in interdigitation as shown in Figure 3.

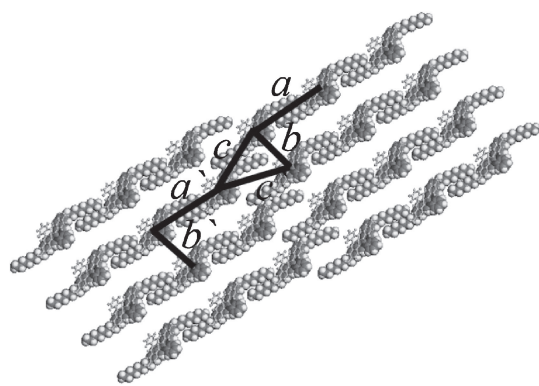


Figure 3. Proposed arrangement for Figure 2a. CPK model is for the underlying layer with adsorbing aromatic rings of B and B' and ball and stick model is for layer with that of A. Octyl chains of ball and stick model are omitted for clarity.

The fact that the ring-like bright spot shown in Figure 2b is similar to that observed for [Ni(2C₁₂-salen)] in which two alkyl chains are introduced at *para*-orientation.³⁵ On the other hand, the STM image of **1** is different from that reported for salphen in which alkyl groups are introduced at *meta*-orientations.³⁴ When four octyl groups are introduced to salphen at both *ortho*- and *para*-positions, a totally different STM image was obtained. Figure 4a shows a 15.0 nm × 15.0 nm STM image of **2** adsorbed on HOPG surface; bias voltage –1.6 V, tunnel current 1.0 nA. The obtained image of **2** is distinct from that of **1** prepared by the same procedure and conditions. The direction of underlying HOPG hexagonal lattice is shown by three lines at the corner.

STM image of **2** shows many bright spots with triangular structure that can be clearly identified as salphen framework covering the whole area. A bright spot with isosceles triangular shape enabled us to distinguish aromatic ring A from the others. Note that the apex of the isosceles triangular image orients toward one of the HOPG lattices. Thus the STM image shows that the molecules are not in the form of dimers as **1**, and the monomeric molecules are lying on the HOPG surface with the molecular plane being parallel to the HOPG surface similarly to other complexes reported. The lengths of the base and the height of a triangle are 1.6 and 1.0 nm, respectively. The size is slightly larger than the actual size of **2**. When viewed along the *a* axis, we can see that the orientation of each complex was inverted alternately, and along the *b* axis, the orientation of every two complexes was inverted. It gives the surface unit cell shown by a rectangle in Figure 4a an expression of plane group *p2gg*, and the unit cell parameter of 4.22 × 2.88 nm², area per unit cell 12.2 nm², and area per molecule 3.04 nm². At a surface, achiral compounds often form chiral domains. However, the obtained STM image of **2** showed only achiral domains.

For a more quantitative representation of the data, the line profile along the *a* axis indicated by an arrow in Figure 4a has been extracted and depicted in Figure 4b. At the center of a single molecule, a hollow due to Ni(II) is observed. Such a hollow is also reported in the STM image of Ni–salphen and phthalocyanine complex.^{25,33} Regarding from one molecule, there are three nearest neighbors, *x* = 1.93 nm (tail to tail), *y* = 1.73 nm (tail to head), and *z* = 1.70 nm (head to head), indicated in Figure 4c. In this model, *para*-octyl groups of a molecule interact by van der Waals interaction with *para*-octyl groups of a neighboring molecule and edges of salphen frameworks of other molecules in contact.

X-ray Structural Analysis. An ORTEP drawn with the atomic numbering scheme of **1** is shown in Figure 5a. The coordination geometry around nickel atom is square-planar N₂O₂, with the ligand coordinated through nitrogen and oxygen atoms in *cis* arrangement. Although the salphen framework is almost planar (maximum deviation from the least-squares average NiN₂O₂ plane is 0.1636(38) Å [C(10)]), three benzene rings are twisted by 4.84(20) [A], 5.34(19)° [B], and 3.48(20)° [B'] to the chelate plane of [Ni(salphen)] framework. The structure observed from *ac* plane in Figure 5b shows that the complexes are stacked in the form of dimers. However, the dimers are linked along the *c* axis by C(sp²)–H...O hydrogen bonds³⁷ and edge-to-face C(sp²)–H... π interaction.³⁷ The geometric parameters of C(sp²)–H...O were 2.64 Å [H(3)...O(1) (*x*, 1.5 – *y*, –0.5 + *z*)], 3.520 Å [C(3)...O(1)], and 157.7° [C(3)–

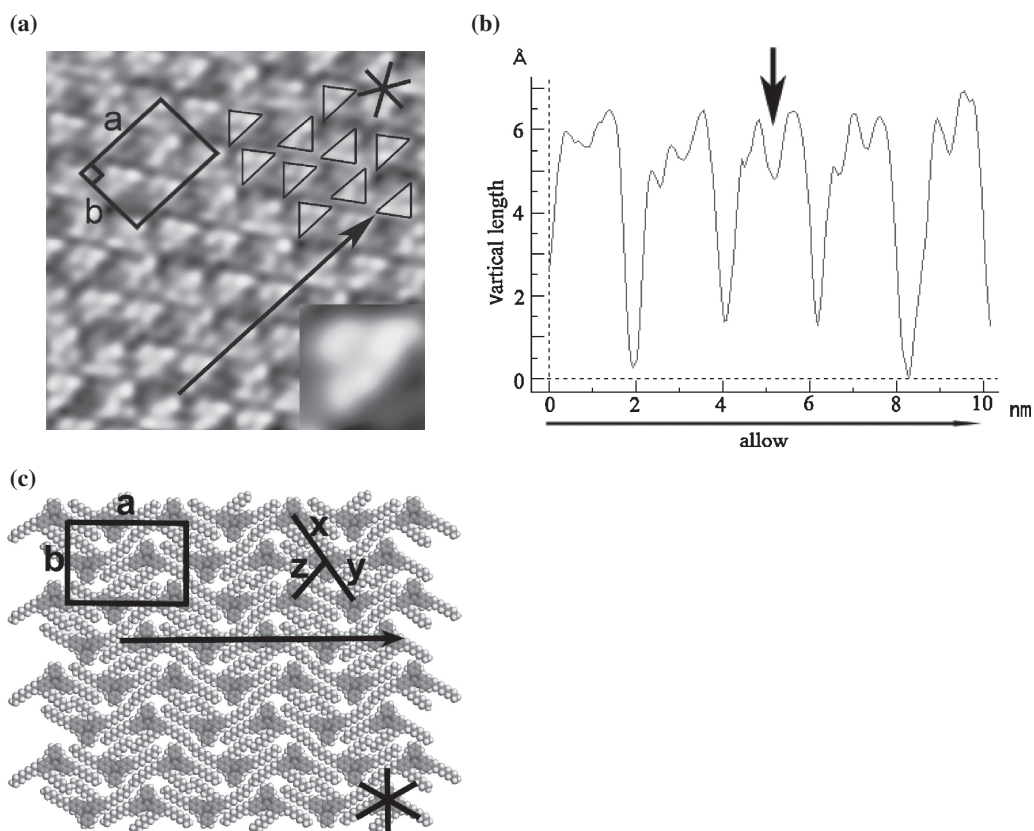


Figure 4. (a) High-resolution STM image of **2** on HOPG. Image area: 15.0 nm \times 15.0 nm; Bias voltage -1.2 V; tunneling current 2.0 nA. Unit cell is plane group $p2gg$ with the unit cell dimensions of $a = 4.22$ nm, $b = 2.88$ nm. (b) Line profile over an arrow indicated in (a). (c) Proposed monolayer model.

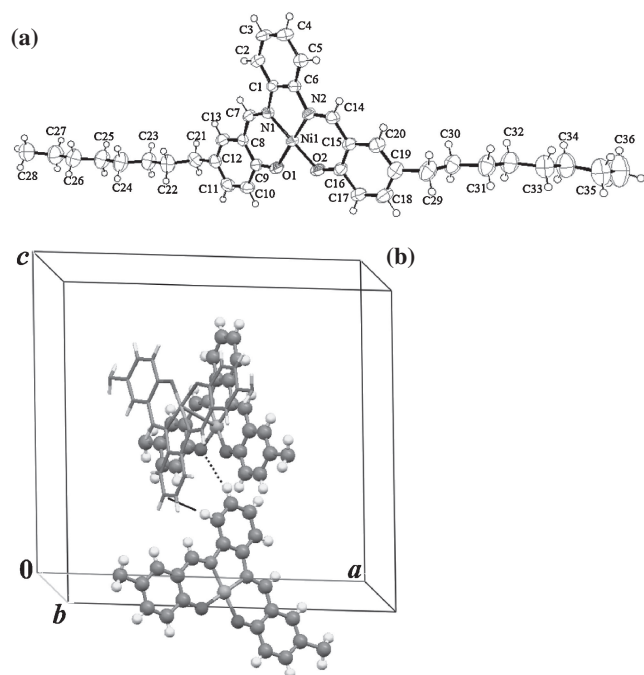


Figure 5. (a) Thermal ellipsoid plot (ORTEP) and atomic numbering scheme of **1**. Ellipsoids are drawn at 50% probability level. (b) Crystal structure of **1**. CH...O (dotted line) and edge-to-face CH/ π (thin line) interactions are also indicated. Octyl chains are omitted for clarity.

H(3) \cdots O(1)], and the edge-to-face distance between C–H of a ring A and the molecular plane of a ring A ($1 - x, 0.5 + y, -0.5 + z$) was 2.996 Å (Figure 5b). Furthermore, the octyl chains of **1** are aligned side by side to form lamellar like structure. Such a structure is commonly observed in crystal of compounds with long alkyl chains. When the crystal structure of **1** is compared with that of the nonsubstituted complex [Ni(salphen)],³⁸ the structure of the dimer is found to be apparently different. On the other hand, the dimer of **1** is similar to [Ni(4*t*Bu-salphen)]³⁹ [H2(4*t*Bu-salphen) = 1,2-bis(3,5-di-*tert*-butyl-2-hydroxybenzimidino)benzene] and [Ni(3,5-Cl₂-saloph)] [H2(3,5-Cl₂saloph) = *N,N'*-1,2-diyl-bis(3,5-dichlorosalicylideneimine)].⁴⁰ Hydrophobic interactions between the octyl groups that lead to form lamellar like structure might be the reason of the difference.

The structure of a dimer of **1** is shown in Figure 6a and the inter- and intradimer arrangements are shown in Figures 6b and 6c, respectively. Intermolecular distance in a dimer is 3.24 Å while interdimer distance is 3.39 Å. The difference is very small, so two arrangements are considered. Four bright spots in the STM image of **1** in Figure 2 are arranged to form hemispherical patterns. It is clear that this pattern accords with the top view of the dimer in Figure 6a.

Dimer Formation in Chloroform-*d* Solution Studied by ¹H NMR. ¹H NMR spectra of **1** and **2** in chloroform-*d* were measured with a 500 MHz spectrometer, and all peaks have been assigned comparing them with those of the reported spectra of the salen analogues. It is known that the ¹H NMR peaks

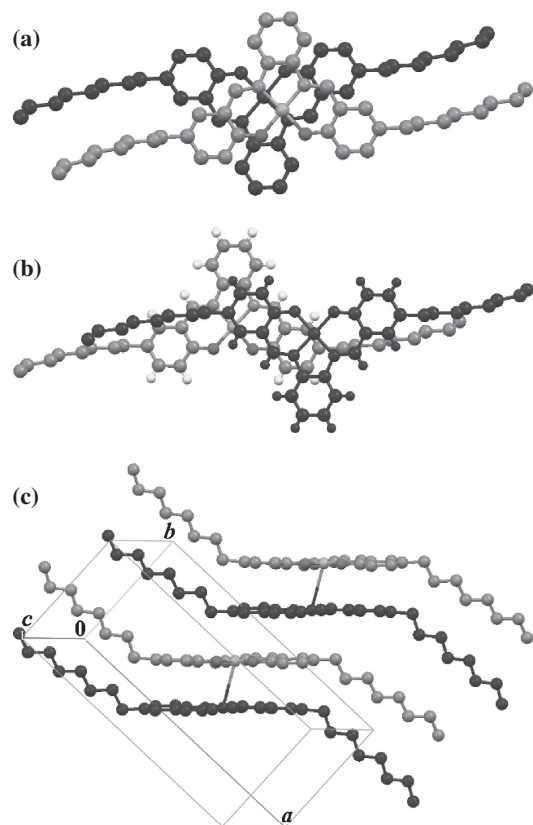


Figure 6. Comparison of dimer and intradimer arrangements. (a) Dimer; top view, (b) intradimer; top view and (c) side view of dimer and intradimer arrangements. Light and dark molecules of (a), and (b) were designed to correspond with (c). H atoms of octyl groups were omitted for clarity.

assigned to Hc and Hd of [Ni(salen)] substituted by alkyl groups exhibit concentration dependence.⁴¹ On increasing the concentration, the signals assigned to the protons Hc and Hd of **1** and **2** also exhibited clear upfield shifts. Figures 7a and 7b show the concentration dependences of Hc and Hd for the **1** and **2**. The shifts were observed only for Hc and Hd, and neither aliphatic protons nor the Ha and Hb protons of the benzene rings showed observable shifts. The proposed structure for the aggregate in chloroform-*d* solution is given in Figure 7c. These upfield shifts became conspicuous above the concentration of ca. 10^{-4} mol L⁻¹, and shifted about a ppm upwards until the solution of **1** and **2** saturated at 40 and 200 mmol L⁻¹, respectively.

As is frequently discussed in the literature, NMR upfield shifts are caused by the approach of an aromatic ring to the protons by aggregation. Although **1** and **2** have an extra aromatic ring *A* compared with the salen analogue, the fact that the same protons exhibit upfield shifts indicates that the structures of the aggregates of **1** and **2** are similar to that of the reported salen analogue.⁴¹ As the ¹H NMR spectra exhibit the shifts and not the splittings, a rapid equilibrium between the aggregate and the monomeric species is indicated. Figure 7a shows that the peak shift of **1** (Hc and Hd) commences from lower concentration than that of **2**. Consequently, the equilibrium constant for the aggregation equilibrium for **1** should be larger than that of **2**. By fitting the data to the following

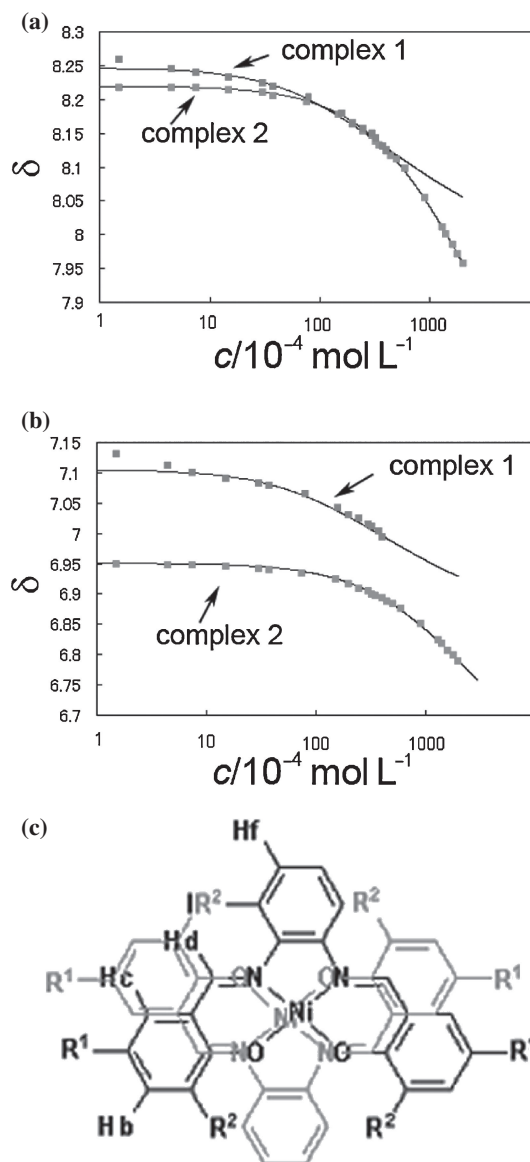


Figure 7. (a) Concentration dependence of Hc and (b) Hd of ¹H NMR position shift in chloroform-*d* solution with calculated curve fitting and (c) proposed aggregation structure of Ni-salphen dimer.

equation which assumes simple monomer–dimer equilibrium, we could evaluate the equilibrium constants for **1** and **2** as 14.5 and 1.9 L mol⁻¹, respectively.

$$\delta = \delta_d + (\delta_m - \delta_d)\{(1 + 8CK)^{1/2} - 1\}/4CK \quad (1)$$

δ , δ_m , δ_d : observed chemical shift, chemical shifts of monomer and dimer, respectively, C : concentration K : equilibrium constant of monomer–dimer equilibrium.

Note that the fitted curves given in Figure 7a agree well with the data. Data obtained from curve fitting are summarized in Table 1.

The results show that the K for **1** is 7 times larger than that of **2**. One reason for the difference is the solubilising effect. The introduction of long alkyl groups increases the solubility toward organic solvent, and the solubility of **2** is 5 times larger

Table 1. Calculated Equilibrium Constants K , and Chemical Shifts of Monomer δ_m , and of Dimer δ_d **1** and **2**

Complex	K /mol ⁻¹ ·L ⁻¹	Hc		Hd	
		δ_m	δ_d	δ_m	δ_d
[Ni(2C8salphen)] (1)	14.5	7.11(6)	6.84	8.25(6)	7.98
[Ni(4C8salphen)] (2)	1.9	6.95	6.47	8.22	7.44
[Ni(2C8salen)] ^{a)}	8	6.81	6.00	7.47	6.25

a) [Ni(2C8salen)] = [N,N'-Bis(5-octylsalicylidene)ethylenediaminato]nickel(II).⁴¹

than that of **1** as mentioned previously. This effect probably stabilizes monomeric **2** in solution, and also leads to the change in surface adsorption behavior.

Conclusion

We have observed change in the surface alignment of [Ni(salphen)] substituted by different number of alkyl groups on HOPG. The increase in the number of substituted long alkyl groups is found to increase the solubility of the complex toward organic solvent, and decrease the tendency to aggregate. This effect is concluded as the reason why **2** with four alkyl groups covered HOPG surface with monomers, while **1** with two alkyl groups covered with dimers.

Experimental

Elemental analyses were performed with a Perkin-Elmer 2400II CHN analyzer. UV-vis-NIR spectra were recorded with a JASCO V-570 UV/VIS/NIR spectrophotometer. IR spectra were obtained with a JASCO FT/IR-410 spectrometer using KBr pellets. All reagents were of reagent grade and used without further purification.

Syntheses. 5-Octylsalicylaldehyde was synthesized by the Reimer-Tiemann reaction⁴² from *p*-octylphenol and chloroform. 3,5-Dioctylsalicylaldehyde was synthesized by the Duff reaction⁴³ from 2,4-octylphenol obtained by the ordinary Friedel-Crafts acylation and Clemensen reduction from *p*-octylphenol and octanoyl chloride, the procedure for which is given elsewhere.

Synthesis of [N,N'-Bis(5-octylsalicylidene)-*o*-phenylene-diaminato]nickel(II) (1**):** Nickel acetate tetrahydrate (0.50 g, 2 mmol) and *o*-phenylenediamine (0.21 g, 2 mmol) were added to 100 mL of ethanol in a flask with stirring. After the solution became red, 5-octylsalicylaldehyde (0.83 g, 4 mmol) was added dropwise to the solution. The reaction mixture was then refluxed for 3 h. Precipitates of **1** formed were filtered and recrystallized from dichloromethane and methanol (1:1) mixed solvents. A single crystal of **1** suitable for X-ray crystallographic analysis was prepared by slow inter-diffusion of *o*-DCB/chloroform (1:1) solution (20 mL) of **1** and ethanol (50 mL) for one week at room temperature. Yield; 2.4 g (90%). Anal. Found: C, 72.36; H, 7.94; N, 4.74%. Calcd for C₃₆H₄₆N₂NiO₂: C, 72.37; H, 7.76; N, 4.69%. ¹H NMR (CDCl₃): δ 0.88 (3H, t, CH₃CH₂-, J = 6.7 Hz), 1.28 (10H, m), 1.57 (2H, m, benzyl-CH₂-CH₂), 2.51 (2H, t, J = 7.6 Hz, benzyl-CH₂), 7.08 (1H, d, J = 1.4 Hz, H_c), 7.10 (1H, d, J = 9.2 Hz, H_a), 7.15 (1H, dd, J = 9.2 and 1.0 Hz, H_b), 7.23 (1H, q, J = 4.0 Hz, H_f), 7.70 (1H, q, J = 4.0 Hz, H_e) 8.22 (1H, s, H_d). UV-vis spectra (1.0 × 10⁻⁴ mol dm⁻³, CHCl₃): ϵ_{\max} (λ_{\max}) = 7768 (493 nm), 5117 (445 nm), and

23981 dm⁻³ mol⁻¹ cm⁻¹ (383 nm). IR spectra; $\nu_{\text{as}}(\text{C}-\text{CH}_3)$ at 2955 cm⁻¹ $\nu_{\text{as}}(\text{CH}_2)$ at 2920 cm⁻¹ $\nu_{\text{as}}(\text{C}=\text{N})$ at 1620 cm⁻¹.

Synthesis of [N,N'-Bis(3,5-dioctylsalicylidene)-*o*-phenylene-diaminato]nickel(II) (2**):** **2** was obtained from 3,5-dioctylsalicylaldehyde by a similar procedure to **1** described above. Yield was 80%. Anal. Found: C, 75.61; H, 9.59; N, 3.59%. Calcd for C₃₆H₄₆N₂NiO₂: C, 75.99; H, 9.49; N, 3.41%. ¹H NMR (CDCl₃): δ 0.88 (6H, *m*-, *o*-, *p*-CH₃CH₂-), 1.29 (20H, *m*), 1.57 (4H, *m*-, *o*-, *p*-benzyl-CH₂-CH₂-), 2.50 (2H, t, J = 7.5 Hz, *p*-benzyl-CH₂-), 2.71 (2H, t, J = 7.5 Hz, *o*-benzyl-CH₂-), 6.94 (1H, d, J = 1.3 Hz, H_c), 7.04 (1H, d, J = 0.9 Hz, H_b), 7.20 (1H, q, J = 3.8 Hz, H_f), 7.68 (1H, q, J = 4.4 Hz, H_e), 8.21 (1H, s, H_d). UV-vis spectra (1.0 × 10⁻⁴ mol dm⁻³, CHCl₃): ϵ_{\max} (λ_{\max}) = 9483 (502 nm), 6457 (456 nm), and 29759 dm⁻³ mol⁻¹ cm⁻¹ (387 nm). IR spectra; $\nu_{\text{as}}(\text{C}-\text{CH}_3)$ at 2955 cm⁻¹ $\nu_{\text{as}}(\text{CH}_2)$ at 2920 cm⁻¹ $\nu_{\text{as}}(\text{C}=\text{N})$ at 1620 cm⁻¹.

STM Measurements. A drop of *o*-DCB 1.0 mM solutions of **1** or **2** was placed on a freshly cleaved surface of HOPG and allowed to settle for a while. Then, this sample was measured by Digital Instruments Nanoscope II/E STM equipment under ambient conditions. Thus, all measurements were performed at the liquid-solid interface. STM tips were prepared by electrochemically etched Pt/Ir(80/20) wire according to reported procedures.²² STM images were obtained with a constant current mode unless indicated. Typically a bias voltage varying from 50 mV to -1.6 V (sample negative) and a tunnelling current of 1.0-4.0 nA were employed. Obtained STM images were manually plane-fit to account for sample tilt and then either low-pass filtered and/or Fourier filtered. By changing the voltage applied to the tip and the average tunnelling current during STM imaging, it was possible to switch from the visualization of the adsorbate layer (high voltage) to that of the underlying HOPG substrate (low voltage). This enabled us to correct the distorted STM image by comparison with the equilateral-triangular lattice of HOPG. The lateral distortion caused by the thermal drift in STM images were calibrated by referencing distortion of underlying graphite lattice measured prior to the molecular image of adlayer. This calibration was carried out by WSxM software.⁴⁴ To distinguish between alkyl groups and aromatic rings, we assigned bright spots as aromatic rings, and slightly bright area as alkyl group. In a usual STM image, aromatic rings tend to appear brighter than alkyl chains because of the presence of π -electrons.

Theoretical Methodology. Optimizing geometry and obtaining orbitals of a single molecule with density function theory (DFT) calculations were carried out using the program package DMol³ in the Materials Studio of Accelrys Inc.⁴⁵ Calculations were performed using the generalized gradient approximation (GGA) proposed by Perdew et al.⁴⁶ (PBE). A double-numeric quality basis set with d-polarization functions (DNP) was used.

X-ray Crystallography. A single crystal of **1** was mounted on a glass capillary. Intensity data were collected at 300(1) K by a Bruker AXS SMART diffractometer equipped with CCD area detector and Mo K α (λ = 0.71073 Å) radiation. The structure of **1** was solved and refined with the SHELX-97⁴⁷ software using direct method and expanded using Fourier techniques. All non-hydrogen atoms were refined anisotropically by the full-matrix least-squares method. Some hydrogen atoms were found from

experimental data directly, and their position and isotropic thermal parameters were refined. Crystallographic data have been deposited at Cambridge Crystallographic Data Centre: Deposit number CCDC-842634 for compound **1**. Copies of the data can be obtained free of charge via <http://www.ccdc.cam.ac.uk/conts/retrieving.html> (or from the Cambridge Crystallographic Data Centre, 12, Union Road, Cambridge, CB2 1EZ, U.K.; FAX: +44 1223 336033; e-mail: deposit@ccdc.cam.ac.uk).

Crystal data for **1**; $M_r = 597.46$; red rectangular block, $0.39 \times 0.10 \times 0.05 \text{ mm}^3$; monoclinic, $P2(1)/c$; $a = 18.867(2) \text{ \AA}$, $b = 9.0908(11) \text{ \AA}$, $c = 18.433(2) \text{ \AA}$, $\gamma = 94.508(2)^\circ$, $V = 3151.7(6) \text{ \AA}^3$, $D_{\text{calcd}} = 1.259 \text{ Mg m}^{-3}$, $2\theta_{\text{max}} = 55.02^\circ$, 18841 reflections collected, 4318 uniques [$R_{\text{(int)}} = 0.0780$]; final GOF = 1.034, $R1 = 0.0813$, $wR2 = 0.1319$, R indices based on 7104 reflections with $I > 2\sigma(I)$, $\mu = 0.649 \text{ mm}^{-1}$.

¹H NMR Measurements. Concentration dependence of ¹H NMR spectra were measured at 25 °C using a lambda spectrometer JEOL JNM-LA500 FT-NMR system. Chloroform-*d* containing 1% TMS as inner reference supplied from Kantoh Chemical Co., was used as a solvent. 5 and 10 mL measuring flasks were used to prepare the sample solution. The solutions of different concentration were prepared stepwise, adding the complex in small portions each time after the measurement had been completed.

Supporting Information

Figure of STM image of large area of **2** on HOPG. This material is available free of charge on the Web at: <http://www.csj.jp/journals/bcsj/>.

References

- G. A. Somorjai, *Chemistry in Two Dimensions: Surfaces*, Cornell University Press, Ithaca NY, **1981**.
- R. Izumi, K. Hayama, K. Hayashi, K. Toko, *Chem. Senses* **2004**, *20*, 50.
- J. Ladd, C. Boozer, Q. Yu, S. Chen, J. Homola, S. Jiang, *Langmuir* **2004**, *20*, 8090.
- S. Huan, G. Shen, R. Yu, *Electroanalysis* **2004**, *16*, 1019.
- F. Maya, A. K. Flatt, M. P. Stewart, D. E. Shen, J. M. Tour, *Chem. Mater.* **2004**, *16*, 2987.
- S. Flink, B. A. Boukamp, A. van den Berg, F. C. J. M. van Veggel, D. N. Reinhoudt, *J. Am. Chem. Soc.* **1998**, *120*, 4652.
- C. P. Collier, G. Mattersteig, E. W. Wong, Y. Luo, K. Beverly, J. Sampaio, F. M. Raymo, J. F. Stoddart, J. R. Heath, *Science* **2000**, *289*, 1172.
- C. M. Whelan, M. Kinsella, H. M. Ho, K. Maex, *J. Electrochem. Soc.* **2004**, *151*, B33.
- Z. Quan, S. Chen, X. Cui, Y. Li, *Corrosion (Houston, TX, U. S.)* **2002**, *58*, 248.
- S. Ramachandran, B.-L. Tsai, M. Blanco, H. Chen, Y. Tang, W. A. Goddard, III, *Langmuir* **1996**, *12*, 6419.
- G. P. Lopez, M. W. Albers, S. L. Schreiber, R. Carroll, E. Peralta, G. M. Whitesides, *J. Am. Chem. Soc.* **1993**, *115*, 5877.
- Q. Zhang, L. A. Archer, *J. Phys. Chem. B* **2003**, *107*, 13123.
- A. Lio, D. H. Charych, M. Salmeron, *J. Phys. Chem. B* **1997**, *101*, 3800.
- V. V. Tsukruk, *Adv. Mater.* **2001**, *13*, 95.
- Y.-S. Shon, S. Lee, R. Colorado, Jr., S. S. Perry, T. R. Lee, *J. Am. Chem. Soc.* **2000**, *122*, 7556.
- M. K. Chaudhury, G. M. Whitesides, *Science* **1992**, *255*, 1230.
- G. M. Whitesides, P. E. Laibinis, *Langmuir* **1990**, *6*, 87.
- C. D. Bain, G. M. Whitesides, *Angew. Chem., Int. Ed. Engl.* **1989**, *28*, 506.
- P. E. Laibinis, R. G. Nuzzo, G. M. Whitesides, *J. Phys. Chem.* **1992**, *96*, 5097.
- R. K. Smith, P. A. Lewis, P. S. Weiss, *Prog. Surf. Sci.* **2004**, *75*, 1.
- A. Ulman, *Thin Solid Films* **1996**, *273*, 48.
- R. H. Lippel, R. J. Wilson, M. D. Miller, Ch. Wöll, S. Chiang, *Phys. Rev. Lett.* **1989**, *62*, 171.
- P. Sautet, C. Joachim, *Surf. Sci.* **1992**, *271*, 387.
- X. Lu, K. W. Hipps, X. D. Wang, U. Mazur, *J. Am. Chem. Soc.* **1996**, *118*, 7197.
- X. Lu, K. W. Hipps, *J. Phys. Chem. B* **1997**, *101*, 5391.
- X. Qiu, C. Wang, Q. Zeng, B. Xu, S. Yin, H. Wang, S. Xu, C. Bai, *J. Am. Chem. Soc.* **2000**, *122*, 5550.
- A. Ogunrinde, K. W. Hipps, L. Scudiero, *Langmuir* **2006**, *22*, 5697.
- S.-L. Yau, Y.-G. Kim, K. Itaya, *J. Phys. Chem. B* **1997**, *101*, 3547.
- T. Ikeda, M. Asakawa, M. Goto, K. Miyake, T. Ishida, T. Shimizu, *Langmuir* **2004**, *20*, 5454.
- R. K. Naqvi, T. B. Melø, B. B. Raju, T. Javorfi, I. Simidjiev, G. Garab, *Spectrochim. Acta, Part A* **1997**, *53*, 2659.
- Y. Kureishi, H. Shiraishi, H. Tamiaki, *J. Electroanal. Chem.* **2001**, *496*, 13.
- H. Kirchhoff, H.-J. Hinz, J. Rösigen, *Biochim. Biophys. Acta, Bioenerg.* **2003**, *1606*, 105.
- M. T. Räisänen, F. Mögele, S. Feodorow, B. Rieger, U. Ziener, M. Leskelä, T. Repo, *Eur. J. Inorg. Chem.* **2007**, 4028.
- T. Fujii, K. Miyamura, *Bull. Chem. Soc. Jpn.* **2000**, *73*, 365.
- I. Sakata, K. Miyamura, *Chem. Commun.* **2003**, 156.
- J. A. A. W. Elemans, S. J. Wezenberg, M. J. J. Coenen, E. C. Escudero-Adán, J. Benet-Buchholz, D. den Boer, S. Speller, A. W. Kleij, S. De Feyter, *Chem. Commun.* **2010**, *46*, 2548.
- G. R. Desiraju, *Acc. Chem. Res.* **1996**, *29*, 441.
- A. Radha, M. Seshasayee, K. Ramalingam, G. Aravamudan, *Acta Crystallogr., Sect. C* **1985**, *41*, 1169.
- O. Rotthaus, O. Jarjays, F. Thomas, C. Philouze, C. P. Del Valle, E. Saint-Aman, J.-L. Pierre, *Chem.—Eur. J.* **2006**, *12*, 2293.
- F. Azevedo, M. A. A. F. de C. T. Carrondo, B. de Castro, M. Convery, D. Domingues, C. Freire, M. T. Duarte, K. Nielsen, I. C. Santos, *Inorg. Chim. Acta* **1994**, *219*, 43.
- K. Miyamura, K. Satoh, Y. Gohshi, *Bull. Chem. Soc. Jpn.* **1989**, *62*, 45.
- I. Fells, E. A. Moelwyn-Hughes, *J. Chem. Soc.* **1959**, 398.
- L. N. Ferguson, *Chem. Rev.* **1946**, *38*, 227, and references cited therein.
- I. Horcas, R. Fernández, J. M. Gómez-Rodríguez, J. Colchero, J. Gómez-Herrero, A. M. Baro, *Rev. Sci. Instrum.* **2007**, *78*, 013705.
- Materials Studio*, version 4.4, Accelrys Inc., San Diego, CA, **2006**.
- J. P. Perdew, K. Burke, M. Ernzerhof, *Phys. Rev. Lett.* **1996**, *77*, 3865.
- G. M. Sheldrick, *SHELX-97 and SHELXL-97, Program for the Solution of Crystal Structures*, University of Göttingen, Germany, **1997**.